JOURNAL OF MATERIALS SCIENCE 14 (1979) 897–919

# Nucleation of recrystallization in compressed aluminium: studies by electron microscopy and Kikuchi diffraction

P. FAIVRE*, R. D. DOHERTY
*School of Engineering and Applied Sciences, University of Sussex, Brighton, UK*

Following the earlier investigation of recrystallization of aluminium by Bellier and Doherty [1] by transmission Kossel diffraction, the details of the nucleation process were studied by transmission electron microscopy and Kikuchi electron diffraction. This showed that nucleation appeared to occur via a sub-grain coalescence process that occurred selectively at deformation bands and at deformation band, grain boundary junctions. Nucleation occurred only at grain boundaries and at deformation bands. The condition for continued growth, of enlarged sub-grains of length $2L$, along the grain boundary $L > 2r(\gamma_s/\gamma_g)$ where $\gamma_s$ is the sub-boundary energy and $\gamma_g$ the grain-boundary energy, was found to be obeyed. The values of the stored energy calculated from the measured sub-grain sizes and misorientations were less than the reported experimental value, indicating that in as-deformed aluminium the dislocation arrays in the sub-boundaries may not have the lowest energy structure assumed in the calculation.

## 1. Introduction

In a recent publication, Bellier and Doherty [1] found by Kossel X-ray diffraction that large local misorientations were developed in compressed coarse-grained aluminium. The main microstructural cause of this misorientation was the "deformation bands" [2] sometimes called "transition bands" [3–5], thin boundaries across which the orientation of one part of a deformed grain changes rapidly to that of a differently oriented part of the same grain. Models of how such deformation bands can arise have been discussed by Dillamore *et al.* [4] in terms of the ideas originally proposed by Taylor [5]. The misorientation develops when different parts of the same grain achieve the same imposed strain by use of different combinations of slip systems, thereby undergoing different crystal rotations. Bellier and Doherty [1] reported deformation band misorientations in aluminium as high as 17° after 20% compression and 40° after 40% compression. On annealing, aluminium with this type of deformed structure gave two types of nucleation processes for recrystallization: strain-induced boundary migration (SIBM) at the pre-existing grain boundaries [6, 7] the sole nucleation mechanism after 20% strain, and grain interior nucleation at deformation bands, the predominant mechanism after 40% strain. The latter nucleation was found by the Kossel orientation measurements [1] to be the deformation band equivalent of SIBM, i.e. the mutual invasion of the two orientations on either side of the deformation band. Bellier and Doherty [1] also reported one other microstructural change, the preferential growth of some sub-grains situated at grain boundaries and at deformation bands. It was suggested that this selective sub-grain growth might be caused in part by sub-grain "coalescence" [3, 8, 9]; the disappearance of *low-angle* sub-boundaries by migration of the dislocations of the sub-boundaries to adjacent higher angled boundaries. As discussed by Li [9] the driving force for such a coalescence process is the lower energy of dislocations in the higher angled boundary. Doherty and Cahn [10]

*Present address: Centre de Recherches, Pechiney BP 24 38540, Voreppe, France.

have used Li's idea to explain the observed preference for sub-grain growth at grain boundaries [1] and deformation bands since, in such regions, adjacent low- and high-angled boundaries would be expected. Enhanced sub-grain coalescence at grain boundaries had been previously reported in a study by transmission electron microscopy (TEM) of deformed and annealed iron [11] and also in lightly deformed alumium alloys [12]. Hu originally observed coalescence at deformation bands in silicon iron crystals [3].

Since the Kossel technique used previously has a limited spatial resolution (5 to 10 $\mu$m) it was decided to try to study the detailed nucleation processes, including the possibility of sub-grain coalescence, in compressed aluminium by TEM. The results of this investigation are the subject of the present paper. In addition to observations of both the deformed and partially annealed aluminium by TEM, the various misorientations were studied in detail by the electron equivalent of Kossel X-ray diffraction, Kikuchi electron diffraction [13].

## 2. Experimental details

Although the original investigation of the deformed structure and the nucleation mechanisms had been carried out with coarse-grained aluminium (800 $\mu$m grain size), it was realized that such material would have too low a nucleation frequency for a successful TEM study. So in order to have a reasonable chance of seeing nucleation in the normally small areas of electron transparent material in thin foils prepared from bulk material, the starting grain size was reduced from 800 $\mu$m to only 80 $\mu$m. This change was achieved by giving material prepared as previously described [1] a final anneal of only 3 min at 400° C rather than 1 h at 550° C. The annealed aluminium cylinders were then compressed to various strains, 20, 40, 60, and 80% reduction in height as previously described, using PTFE lubrication to achieve as homogeneous a strain as possible. Annealing was carried out in temperature-controlled salt baths to ensure rapid heat up to the annealing temperature. For optical and electron metallography, the samples were sectioned, parallel to the compression axis, by spark machining at the slowest cutting speed. The depth of damage produced by spark machining was estimated to be less than 50 $\mu$m since thin foils prepared from 100 $\mu$m spark-cut samples showed no dislocations within the recrystallized grains while damage was seen in foils initially only 80 $\mu$m thick. For optical examination the spark cut surface was ground down by some 20 $\mu$m and electropolished to remove a further 50 $\mu$m and the surface then anodized and examined with polarized light.

The samples for TEM investigation were prepared by a method suggested by Pond [14] that enabled large electron transparent areas, up to 1 mm diameter, to be produced. The ability to examine such large areas was vital in a TEM study of such a hetereogeneous phenomenon as nucleation in moderately deformed material. The method used was to cut slices 250 $\mu$m thick and 5 mm square by spark machining from either deformed material or material that had been lightly annealed in bulk before sectioning. Both sides of the spark machined slice were ground down to give a thickness of about 200 $\mu$m and the slice was then thinned by a modified Bollman technique [15].

The thin foil samples were examined in an AEI EM6G microscope at 100 kV. Interesting areas were selected, photographically recorded at low and moderate magnifications and the plates were developed and printed. The prints were used both as a guide and also to record the individual sub-grains whose orientations were measured by Kikuchi electron diffraction. The diffraction patterns were obtained using selected-area apertures of 10 and 25 $\mu$m diameter giving areas on the sample of 0.2 and 0.5 $\mu$m size. Using the following relationship [16] for the estimated positional error $\Delta$, in terms of the spherical aberration coefficient $C_s$ and the Bragg angle $\theta$,

$$\Delta = 8C_s\theta^3$$

gives with $C_s$ of 3 mm and $\theta$ of 0.01 radians,

$$\Delta = 0.03\,\mu\text{m}.$$

An exposure time of about 30 sec was normally found sufficient to give good quality Kikuchi patterns – presumably due to the well recovered cell structure in as-deformed, pure aluminium. Care was taken once an area was being studied to make no change in the specimen orientation. The methods used for indexing the Kikuchi lines, measuring the orientation of individual sub-grains and for determining the misorientation between individual sub-grains have previously been described by Faivre [17]. The results are quoted here as the angle of rotation about whichever of the 24

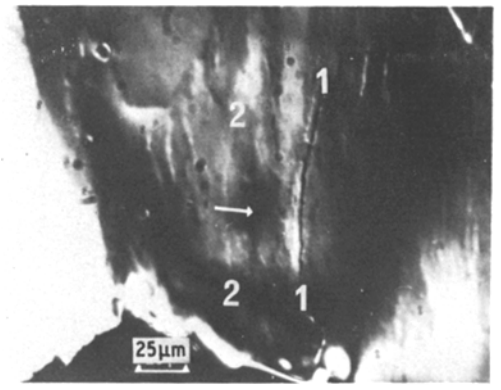


*Figure 1* Optical micrograph of electropolished TEM foil after electron microscope examination. The compression axis is almost horizontal.

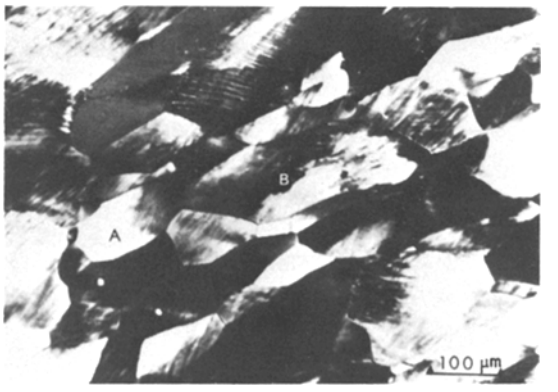


*Figure 2* Aluminium deformed 40%, section parallel to the compression axis seen by polarized light.

possible rotation axes (cubic crystals) gives the smallest misorientation. As described by Faivre [17], this sometimes involved calculating all 24 possible angle/axis pairs; however, this was normally not necessary for most of the smaller misorientations.

It had been originally hoped that thin foils could be produced from interesting areas previously chosed by optical microscopy. This proved unsuccessful in the present investigation, though subsequently a successful technique for achieving this was developed [18]. However, at the end of the investigation when it was necessary to try to discover whether or not the highly misoriented regions giving rise to nucleation were at pre-existing grain boundaries. The question was answered by examination of the TEM foils by optical microscopy. The contrast available using interference techniques on the as-polished samples was sufficient to identify pre-existing grain boundaries (Fig. 1). The blackened contamination spot, arrowed, can be seen to be between a clearly etched grain boundary, 1–1, on the right and a less clearly visible grain boundary, the white line, 2–2, on the left.

Finally, some very brief observations were also made on heavily cold-rolled commercial aluminium foil by the TEM and Kikuchi methods both on the as-deformed material and after a brief anneal.

## 3. Experimental results

### 3.1. Optical microscopy

#### *3.1.1. As-deformed material*

Sections cut parallel to the compression axis for material deformed 40 and 60% are seen in Figs. 2

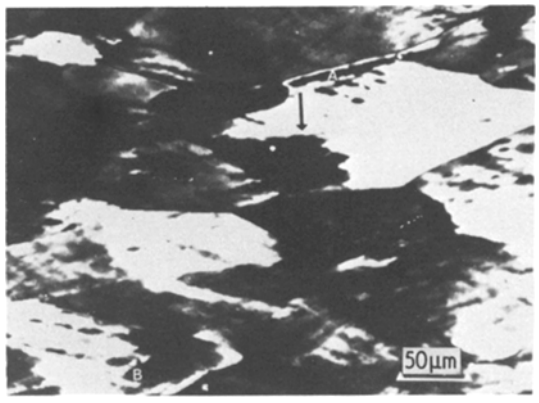


*Figure 3* Aluminium deformed 60%, section parallel to the compression axis. The compression axis is vertical.

and 3. The structures show the original grains that are apparently undergoing the same shape change as the specimen. With the small grain size of 80 $\mu$m, after strains of 60% reduction in height, the "pancake" shaped grains are on average, only 32 $\mu$m thick. For this reason sections for examination in both optical and electron microscopy were taken with the compression axis parallel to the section in order to see as many grain boundaries as possible [19] and to reduce the confusion due to grains nucleating just above and below the plane of section and therefore bringing orientations not visible in the deformed material into the field of view [1]. In the lightly deformed material, 20 and 40%, some grains, e.g. grain A in Fig. 2, were seen with quite uniform shading at all rotations of the specimen with respect to the polarization axis. For most other grains, for example B in Fig. 2 and as indicated by the arrow in Fig. 3, very sharp changes

of shading could be seen – the deformation bands previously reported by Bellier and Doherty [1] in compressed aluminium and by Inokuti and Doherty [20, 21] in iron. The structures seen in the compressed, fine grain size, aluminium in the present work are very similar to those reported for the larger grain size material [1] with perhaps slightly fewer deformation bands per grain in the finer grain size aluminium. With increasing strain, to 60 and 80%, the grain interior misorientations become sharper as indicated by the arrow in Fig. 3 with high sub-grain contrast also developing (A and B in Fig. 3), though this was found to be at close to the resolution limit of the polarized light technique. For the material compressed 80%, the flattening of the grains and the increase of grain interior contrast made it almost impossible to make out the details of the grain and deformation band structure by optical microscopy. In both Fig. 2 and Fig. 3 some indication of the "columnar structure" seen by TEM (Section 4.1) can be made out.

### 3.1.2. Partially annealed material

The fraction recrystalized, $X_v$, was measured for the 80 $\mu$m grain size material by a point counting technique [22] for comparison with that obtained earlier for the coarser grain size material [23]. The results are given in the conventional plot, using Equation 1 [24], Fig. 4.

$$X_v = 1 - \exp(-kt^n)$$

$$\log.\log.\left(\frac{1}{1-X_v}\right) = \log k + n \log t. \qquad (1)$$

$X_v$ is the fraction recrystallized as a function of annealing time $t$ and $k$ and $n$ numerical constants.

The results show the very great enhancement of the recrystallization rate at 328° C with the reduction of the existing grain size. It is also noticeable that the exponent changes from $n = 1$ at 20% strain (800 $\mu$m) to $n$ of between 1.5 and 1.9 for the other materials. Cahn [25] has discussed the possible significance of different values of $n$. A value of 1 for $n$ would be expected for nuclei forming along the area of grain boundaries and growing at a constant rate into the grains, giving an initially constant rate of *volume* increase with time. This interpretation is compatible with the observations reported by Bellier and Doherty [1] of *colonies* of new grains forming by SIBM, after 20% strain. In the present work, with the

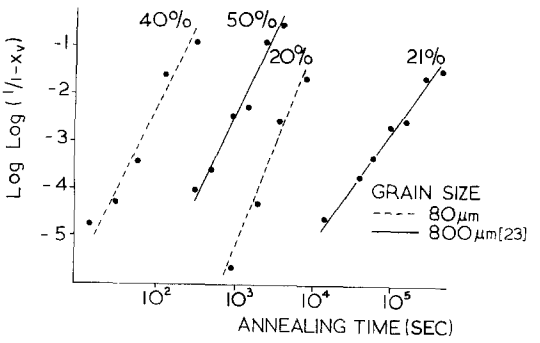


*Figure 4* Volume fraction recrystallized, $X_v$ as a function of annealing time at 328° C after different amounts of compression.

finer grain size, only *individual* SIBM bulges were seen (Figs. 5 and 6) so that an initially accelerating rate of volume recrystallized would be expected, giving a higher value of $n$.

Fig. 5 shows various examples of nucleation by SIBM bulges, in material strained 20%. The individual bulges are indicated by arrows, though with the variable contrast produced in the image some of the bulges are not easily visible in the specimen rotation position shown. It can also be seen that many of the grains show apparent deformation bands (Figs. 5 and 6). Of interest is the central white grain in Fig. 5, which has produced several SIBM bulges in a region associated with a faint horizontal deformation band *within the parent grain.* The small highly contrasty grain at the upper right can also be seen to be giving rise to SIBM bulges, indicated by white arrows. Other examples of the association of SIBM with "parent" grain misorientations were found [15]. Material briefly annealed at 328° C after 40% compression

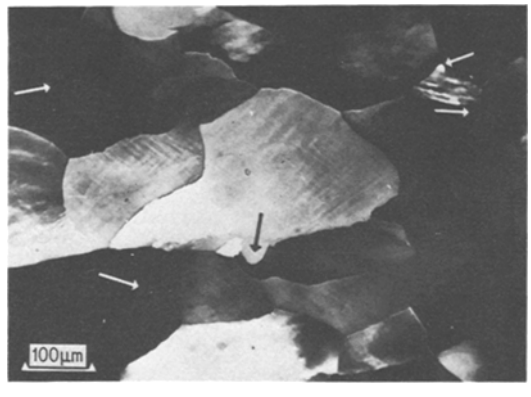


*Figure 5* Aluminium compressed 20% and annealed for 30 min at 328° C.

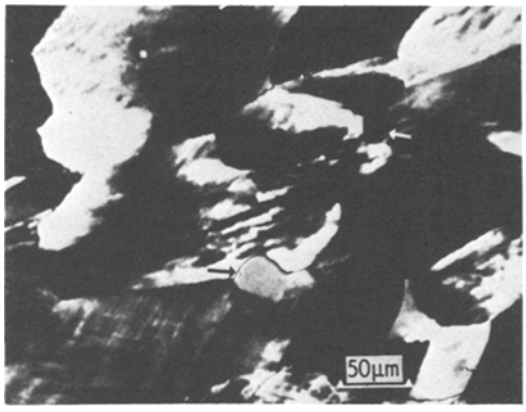


*Figure 6* Aluminium compressed 40% and annealed for 5 min at 328° C.

also showed predominantly SIBM nucleation (arrows in Fig. 6), with little evidence of the deformation band nucleation in grain interiors, that had been reported for 800 μm grain size material compressed 40% [1]. It is noticeable in Fig. 6 how the bulge indicated by the black arrow appears to show the growth *within the parent grain* which had been previously reported [1]. It may also be seen that the position in the parent grain where this growth has occurred is close to a small area showing a different, white, constrast (just to the right of the bulge), indicating nucleation at deformation band between the two different parent grain orientations. The upper bulge, indicated by the white arrow, also seems to be associated with the black/white deformation banding in the parent grain.

For more heavily deformed material, 60 and 80% compression, the recrystallization occurred rapidly so that the annealing temperature had to be reduced to only 250° C. Fig. 7 shows material

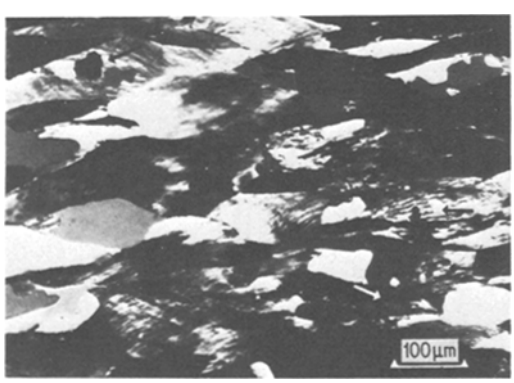


*Figure 7* Compresssed 60% and annealed for 2 min at 250° C.

partially recrystallized after 60% compression, with many nuclei at the grain boundaries but also, as indicated by the arrows, new grains formed by *grain interior* nucleation. The fine scale and complexity of the deformed structure precluded, however, any serious study of nucleation by optical microscopy after high strain. This was even more true for material deformed 80% [15].

## 4. Electron microscopy

Since the optical microscope had shown that the change from grain boundary, SIBM, nucleation to mainly grain interior nucleation took place between 40% and 60% compression, material deformed by these amounts was chosen for detailed examination by TEM. 30 samples of material strained to these amounts were examined in both the as-deformed and partially recrystallized state with the orientations of a total of 1200 sub-grains determined by Kikuchi electron diffraction.

### 4.1. As-deformed material

#### *4.1.1. Material compressed 40%*

Although the optical microscope had found deformation bands in almost every grain; the electron microscope did not reveal, either by different sub-grain shape or by enhanced sub-grain contrast, the position of these deformation bands. In an average 80 μm size grain, well over 3000 sub-grains were visible and short of determining the orientation of a significant fraction of these sub-grains, no way of identifying the deformation bands could be found. Random areas were, therefore, selected and these were examined in detail. Fig. 8 shows regions within grains and Fig. 9 shows a grain boundary triple point, the junction of three grains. The sub-grains, in the section seen, vary from about 0.5 to 5 μm in size with some tendency to a columnar alignment in some of the grain interior regions (Fig. 8). These columns often appeared to be closely parallel to the {1 1 1} slip planes. The inclination of these colums varied from grain to grain but was always within 30° of the compression plane (see Fig. 3). The sub-grain shape was consistently more equi-axed near grain boundaries (Fig. 9), but with no consistent difference in sub-grain *size* between grain boundary and grain interior regions. There was, however, a somewhat greater average misorientation of 4.7° (with a standard deviation of 2.7°) of the sub-boundaries at the grain-boundary regions, than

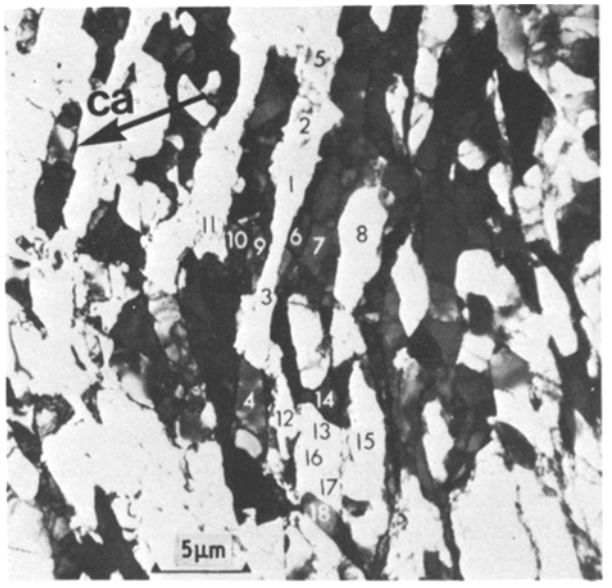


*Figure 8* Material compressed 40%. The compression axis, ca, is indicated.

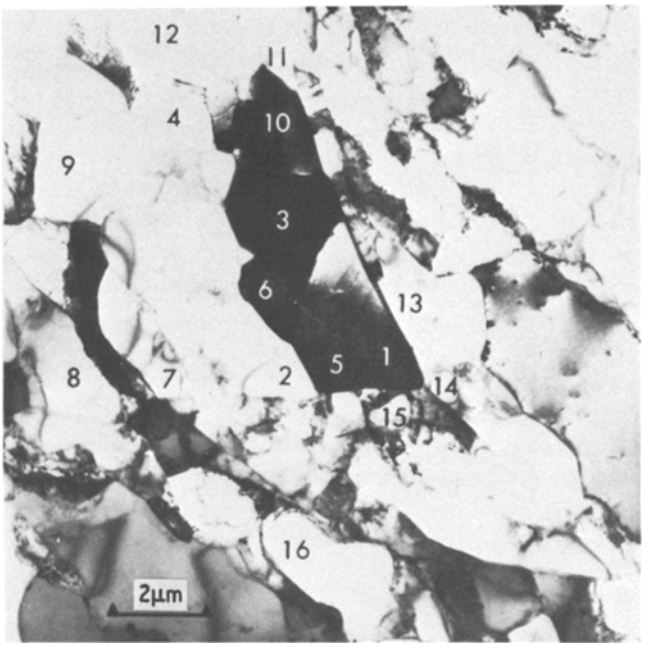


*Figure 9* Material compressed 40%. Subgrains 1, 14 and 15 are all in different grains.

within the grain interiors where the mean sub-boundary misorientation was only 2.9° (±2.5°).

The sub-grains along the columns, in Fig. 8, have quite small misorientations, e.g. 5/2 0.7°, 2/1 2.7°, 1/3 2.7°, 14/13 1.1°, 13/16 1.1°, 16/17 0.1°, 17/18 2.9°. Across the columns many, but not all, the misorientations are larger. Sub-grain 1 is rotated away from both its neighbours 9 and 6 by 4°, about [2 1 2], but the rotation is not continuous as 9 and 6 are only misoriented by 1° from each other. The misorientations across the lower column are also quite large 15/13 − 8.1°, about an axis near [2 1 2], 13/12 + 7.2° also about [2 1 2] and finally 12/4 − 5.7° about the same axis. Since the sign of the rotation angle is changing it is clear that there is no consistent rotation as would occur at a deformation band [3]; sub-grains 12 and 15 are only misoriented by 1.2°. Not all the sub-boundaries parallel to the column structure have higher than normal angles as can be seen from the

following sequence of misorientations: 8/7 0.7°, 7/6 1.2°, 9/10 2.5°, 10/11 4°.

Fig. 9 shows the microstructure at a triple point. Sub-grains 1, 14 and 15 are all in different grains. (1/14 − 55° about an axis close to [1 1 1], 14/15 + 57° about an axis close to [$\bar{1}$ 4 1] and 15/1 + 56° about [2 $\bar{1}$ 2].) Some of the sub-boundaries have small angles such as 5/1 0.6° and 1/3 1.1°, with most of the other angles only 4° to 6°, apart from 11/12 12° about [$\bar{3}$ 1 $\bar{1}$], 12/4 9.8° about [1 $\bar{2}$ $\bar{1}$] and in the adjacent grain 14/13 7.7° about [2 2 1]. Although the structures do not indicate any form of deformation banding it would appear that, at grain boundary triple point regions, the combination of low- and high-angle boundaries needed for coalescence do appear to exist with, in addition, occasional much higher than normal angles, at *sub-boundaries* being found *within* the grains.

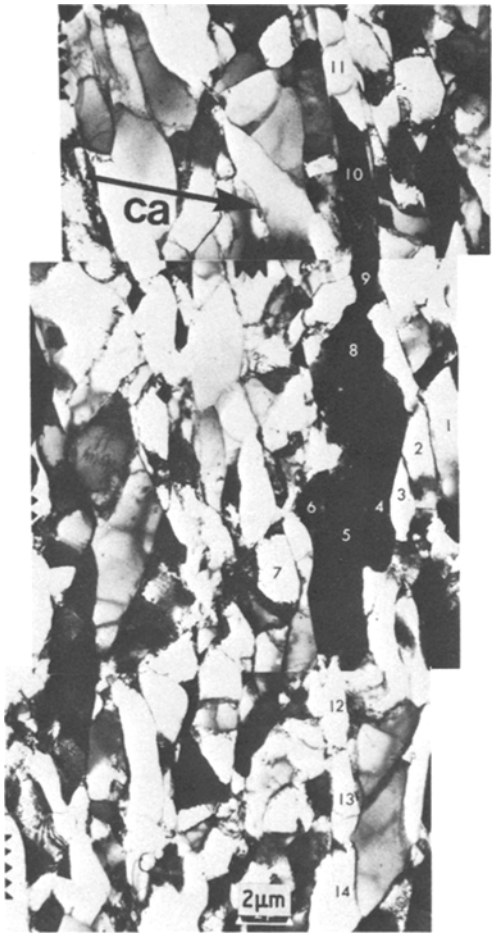


*Figure 10* Aluminium compressed 60% with the compression axis, ca, shown.

### *4.1.2. Material compressed 60%*

The elongated, columnar structure seen in material deformed 40% (Fig. 8), was further developed after the higher strain (Fig. 10). The columns were again found to lie close (within 10°) of a {1 1 1} slip plane and to be normally within 30° of the compression axis. The structure of the original grain boundaries are now much more difficult to make out than they were after the lower strain and there was again no way that was found for detecting the sharp deformation bands known to exist from the optical microscopic observations (Fig. 3).

Fig. 10 is a fairly typical field of view showing the columnar sub-grains, with in general low misorientations along the column, 11 to 14. The misorientations were: 11/10 2.8°, 10/9 0.8°, 9/8 1.1°, 8/5 3.3°, 5/12 4.8°, 12/13 0.6°, 13/14 6.4° but with a total misorientation of only 1.3° along the whole column 11 to 14. Across the column the individual angles were somewhat larger: 1/2 3°, 2/3 − 6.9°, 3/4 3.5°, 4/5 2.1°, 5/6 − 3.1°, 6/7 4.4° about rotation axes that were all between [$\bar{2}$ $\bar{1}$ 2] and [0 1 1]. The angles were not cumulative however, showing that this column was not a deformation band; there being, between 1 and 7, a total misorientation of only 6.4°.

The region shown in Fig. 11 does not have the columnar structure but very large misorientations were found:

| | |
|---|---|
| 8/7 | 19° about [1 1 2] |
| 5/6 | 18° about [1 1 2] |
| 10/11 | 11° about [2 1 2] |
| 13/14 | −14° about [1 1 2] |
| 14/15 | 22° about [1 2 2] |
| 13/18 | −10° about [2 1 3]. |

Despite these high and irregular misorientations and the irregular shape of the interface between the two orientations, it is not certain if this is a medium-angle grain boundary or a deformation band, as no clear indication could be found of intermediate orientations characteristic of well developed deformation bands [3, 4].

One remarkable structure was seen, (Fig. 12). This showed two enlarged sub-grains 3 and 8 which were much larger than their neighbours and had many high-angle boundaries. These are the


*Figure 11* Aluminium compressed 60%.

characteristics required of a recrystallization nucleus [27] despite the fact that the sample had not been annealed above room temperature. The high-angle boundaries seen included the following:

| | | |
|---|---|---|
| | 2/3 | 39° about $[2\,\bar{2}\,1]$ |
| | 3/4 | 45° about $[2\,\bar{2}\,1]$ |
| | 9/8 | 27° about $[1\,\bar{2}\,1]$ |
| | 8/7 | 33° about [1 1 2] |
| and | 30/31 | 54° about [3 1 3]. |

The structure is very confused with no clear single high-angle interface and no unique rotation axis. There appear to be 4 or 5 bands of separately oriented groups of sub-grains intermixed in a complicated way. The following groups of simlarly oriented sub-grains could be found:

(i) 31, 6, 32, 13, 33, 9, 10, 22, 23

(ii) 8, 12, 11, 14, 15, 16

(iii) 3, 24, 20, 18, 17

(iv) 1, 2, 29, 4, 5

and (v) 7, 30, 19

Each group had a range of small to medium misorientations (0.5 to 14°) between the members of the same group and larger angles (>20°) about different rotation axes between the different


*Figure 12* Material compressed 60%.

groups. There were a few particularly low-angle boundaries found:

6/32 0.5°, 8/12 1.5°, 7/30 1.6°, and 3/24 1.8°.

Sub-grain 3 was completely free of any dislocation sub-structure, while sub-grain 8 contained only a few dislocations. The appearance of the apparently well-formed recrystallization nuclei after room temperature deformation may be compared with the report by Cairns *et al.* [26] that heavily drawn copper wire shows dynamic recrystallization during room temperature deformation.

## 4.2. Partially recrystallized material

### *4.2.1. 40% compressed material*

The most striking example of pre-nucleation sub-grain development in this study has already been published in review articles, Fig. 15 of [27] and Fig. 24 of [28], and need not be reproduced here. This previously published micrograph showed clear evidence for sub-grain coalescence but only at a singular position – the junction of a deformation band and a high-angle grain boundary. The groups of coalesced sub-grains lay *within the grain* containing the deformation band; that consisted of material misoriented by 8 to 13° from material on either side; however, the rotations about a similar

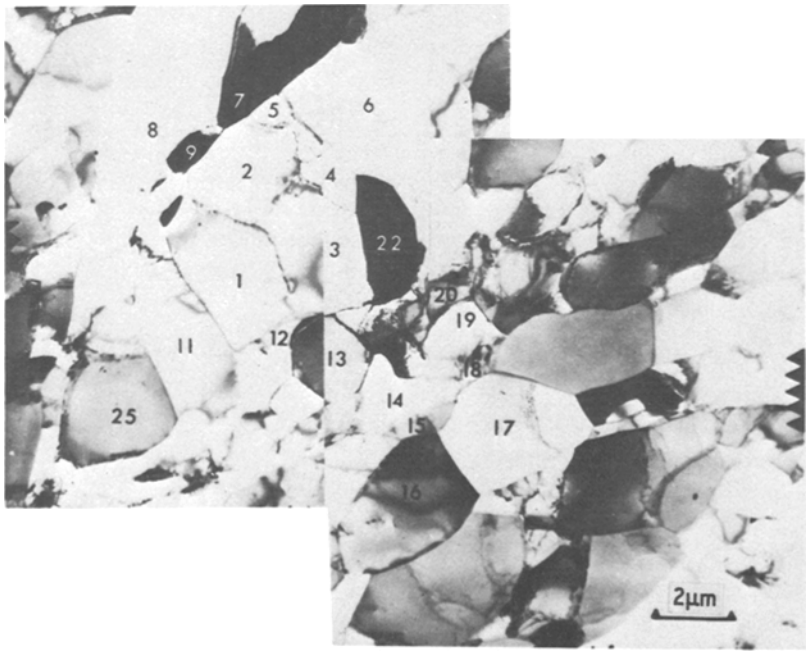


*Figure 13* Aluminium compressed 40% and annealed for 10 sec at 328° C.

axis being of an opposite sense, were not cumulative [15].

Another group of apparently coalescing sub-grains in the same sample, lightly annealed for only 10 sec at 328° C, is seen in Fig. 13. Sub-grains 1 to 5 are all very close in orientation:

$$1/2\ 0.2^\circ$$
$$2/3\ 0.1^\circ$$
$$3/4\ 0.4^\circ$$
$$2/5\ 0.6^\circ$$

Unlike the previous case of sub-grain coalescence discussed above and shown in [27, 28], the surrounding sub-boundaries *in the plane of the foil* are of low to medium angle, 2° between 2/9, 4/6 and 1/11, 3° 1/12 and only 1.2° 4/22. There are some nearby higher angles:

$$18/17\ 7.8^\circ \text{ about } [0\,2\,1]$$
$$17/16\ 5.4^\circ \text{ about } [\bar{1}\,0\,0]$$
$$15/14\ 5.1^\circ \text{ about } [\bar{1}\,1\,1]$$
$$11/25\ 4.7^\circ \text{ about } [\bar{2}\,1\,1]$$

and the sub-grains to the left of 8 and 25 belong to a different grain, so that there is again a nearby high-angle grain boundary. Although in this example there is no contact between the apparently coalescing group of sub-grains and either the grain boundary or any above average misoriented sub-boundaries in the section of the foil, such contact with high-angled boundaries is, however, possible above or below the foil. (The sample, like all others, was annealed in the bulk and then thinned.)

In order to see if such enlarged groups of sub-grains lying at, or close to, pre-existing grain boundaries could give rise, as predicted [10], to nucleation by SIBM; material was examined after a somewhat longer anneal, 30 sec at 328° C. Examples of grain-boundary nucleation are shown in Fig. 14 to 17.

In Fig. 14, a grain boundary lies as indicated by the dashed lines between the regions marked as I and II, with enlarged sub-grains lying within grain II, but just starting to bulge into grain I. The fact that these sub-grains are elongated more along the boundary, towards 8 and towards 4, than elongated into I, suggests a within-grain coalescence process [10]. This hypothesis is supported by the large misorientation, 18° about $[1\,\bar{2}\,4]$, between 1

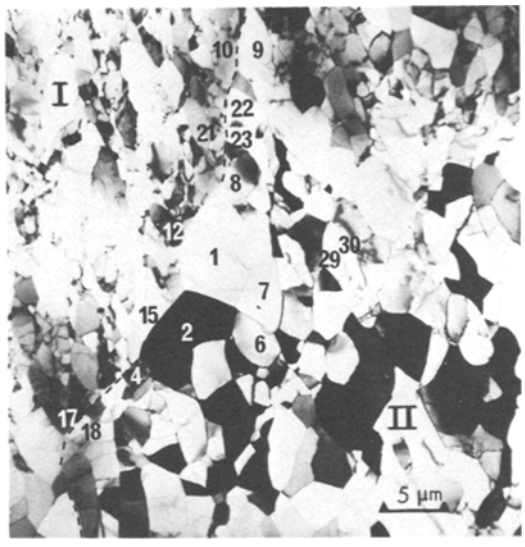


*Figure 14* Aluminium compressed 40% and annealed for 30 sec at 328° C.

and 2, and 16° between 6 and 7, which are also larger than average size. This misorientation appears to be a deformation band rather than a pre-existing grain boundary since other large misorientations are:

$$1/29 \quad -21^\circ \text{ about } [0\,\bar{1}]$$
$$29/30 \quad 20^\circ \text{ about } [0\,\bar{3}\,3]$$
$$18/1 \quad -29^\circ \text{ about } [1\,\bar{3}\,4]$$
$$1/23 \quad -10^\circ \text{ about } [0\,\bar{1}\,2].$$

The irregular shape of the misoriented boundary and the fact that the misorientation changes progressively from 18 to 1 and then the further misorientation from 1 to 23 is in the opposite sense, indicates that the nucleation has occurred at a junction of a deformation band within grain II rather than at a pre-existing triple point. The misorientation between grains II and I changes as follows:

$$18/17 \quad 44^\circ \text{ about } [1\,\bar{3}\,2]$$
$$2/15 \quad 33^\circ \text{ about } [1\,\bar{3}\,2]$$
$$1/12 \quad 20^\circ \text{ about } [1\,\bar{3}\,1]$$
$$\left.\begin{matrix}23/21\\9/10\end{matrix}\right\} \ 30^\circ \text{ about } [1\,\bar{3}\,2],$$

again indicating that the orientation of 1 has changed with respect to material 18, 2 and 23 on either side of 1. Sub-grains 22 and 23 have practi-

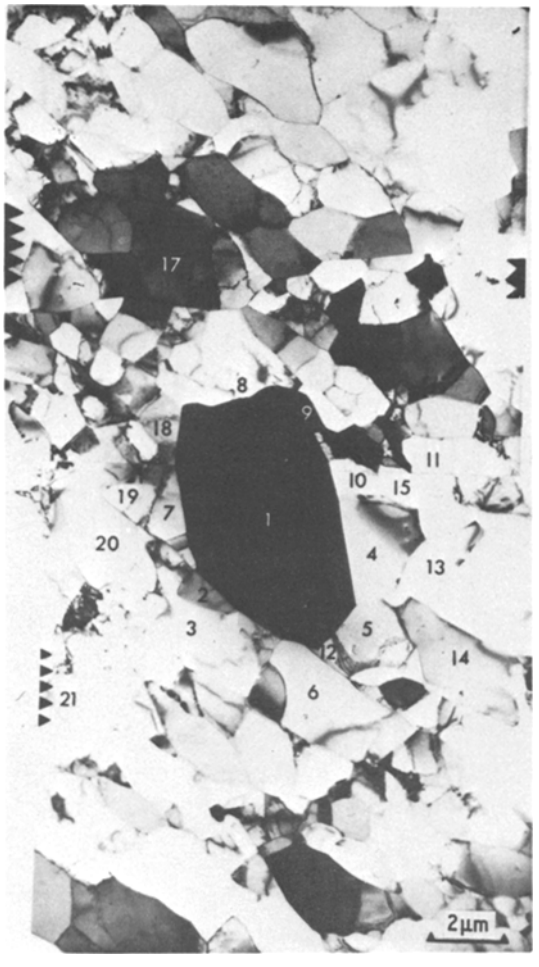


*Figure 15* Aluminium compressed 40% and annealed for 30 sec at 328° C.

cally coalesced (0.4° misorientation) and this region is starting to grow into 21.

In Fig. 15 a greatly enlarged sub-grain, 1, is seen within a region that was apparently a single grain before deformation. There are two pre-existing grain boundaries in the region seen, one separates the region around sub-grain 1 from the lower grain that includes sub-grains 20, 2, 3, 6 and 21, the other boundary runs, almost horizontally, across the micrograph just beneath sub-grain 17. The triple point, the meeting point of the grain boundaries, lies just off the left-hand side of the micrograph, beneath the upper of the two black left-hand plate-locating marks. The foil had been tilted to put the enlarged sub-grain in maximum contrast, however, even in other foil orientations, no dislocations or low-angle boundaries could be seen within sub-grain 1. The orientation of sub-grain 1 is within 6° of a group A of sub-grains 8, 9, 10, 15, 4 and 13, but is strongly misoriented from 2 other groups of sub-grains: group B 11, 5, 12 and 14, and group C 7, 18 and 19. From sub-grain 1 to sub-grain group B is a rotation of 10 to 20° about an axis close to [1 0 0] and from 1 to C is 18° about an axis near to [1 2 0]. There appears to be a quite complicated system of deformation bands within the grain near the triple point and it is within this network of bands that the enlarged sub-grain has developed. Only after this within-grain process, has the resulting nucleus just started to bulge into the lower grain, consuming the sub-grains between 2 and 6. Since sub-grain 1 has grown so large within its own grain it is difficult to decide by what processes it might have grown to this observed size. However, it might be noticed that sub-grains 13, 14, 5 and perhaps 4 appear to be growing or to have grown by coalescence – as shown by the remnants of sub-boundaries within the enlarged sub-grains. These almost vanishing low-angle boundaries are causing almost no cusping on the adjacent boundaries. As sub-grains 4 and 13 (group A) are strongly misoriented from adjacent sub-grains, 11, 5 and 14 (group B), this apparent coalescence has occurred in the neighbourhood of local deformation bands with 10 to 20° misorientation and again close to a grain boundary.

A fully developed SIBM nucleation even is seen in Fig. 16, where a new grain 1 with an orientation similar to some of the lower sub-grains is migrating into the upper grain. The high-angle grain boundary runs on the right-hand side between 7 and 8 (44° misorientation about an axis close to [1 2 2]) and on the left-hand side between 4 and 21 (36° [1 2 1]). The misorientation between 1 and the surrounding sub-grains 9 to 21 is approximately 40° (± 6°) about an axis that varies between [1 2 1] and [1 1 1]. The misorientation, moreover, is of 38° to 43° about an axis very close to [1 1 1] between 1 and sub-grains, 18, 19, 5, 20, 6 and 21. It may be seen that the bulge has distorted towards these sub-grains – as would be expected since a grain boundary, with a misorientation of 40° about [1 1 1], is a high mobility boundary [29, 30]. With respect to the lower "parent" grain, the SIBM "daughter" grain has a range of misorientations that varies; being only 2° from 24, 3.5° from 23, 4° from 7, 5° from 22, 9° from 4 and 13° from 25. Sub-grain 25, therefore, quite strongly misoriented from its surrounding sub-

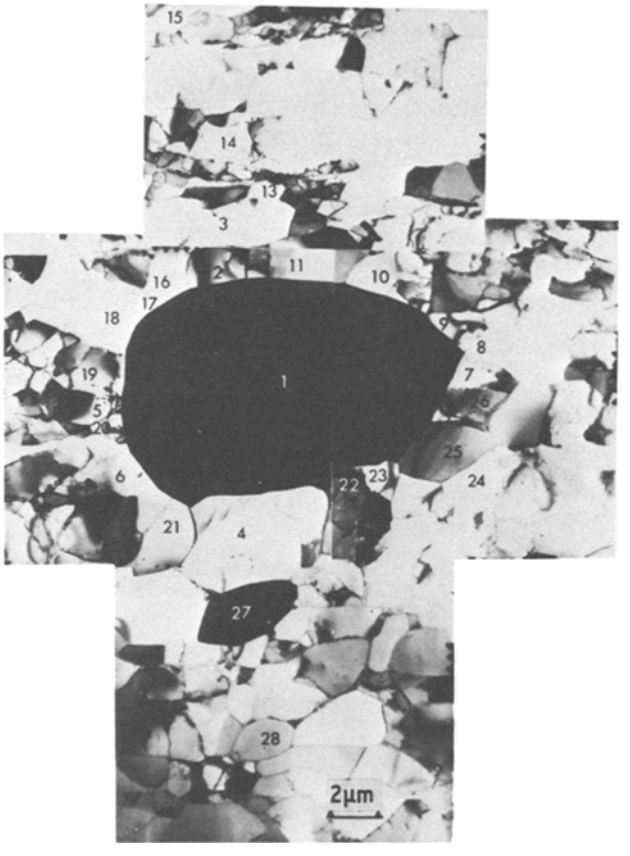


*Figure 16* Aluminium compressed 40% and annealed for 30 sec at 328° C.

grains, 9° from 26 and 13° from 23 though only 2° from 24. These high local misorientations found in the lower parent grain suggest an incipient deformation band in this region but again one in which the orientation changes from that of 7 and 26 to that of 25 and 24 before swinging back to 22 and 23 which have similar orientations to 7, 26 and 1. There is no direct metallographic evidence that supports sub-grain coalescence as a preliminary process in the initial development of the new grain. However, since the new grain is now some 14 $\mu$m in size, in the plane of the foil, it is very unlikely that the initial sub-grain or group of sub-grains from which the new grain developed would have been within the foil thickness. Some evidence for a coalescence process can, however, be seen in the enlarged sub-grain 4 and also between 7 and 26 which are misoriented by only 0.2°. Both these regions are situated at the pre-existing high-angle grain boundary and are next to quite high local misorientations of 5 to 10°.

The most fully developed recrystallized grain investigated, after 40% compression, is shown in Fig. 17. In the micrograph four original grains are present. The parent grain from which the recrystallized grain (12, 13) has developed includes sub-grains 8, 39, 29, 41, 31, 32, 34 as well as 1, 2, 3, 4, 5, 6 and 7, 12/13 is only 7° from 32. The 3 other grains are as follows: firstly, there is a grain in the lower left that includes sub-grains 35 and 20 this is misorientated by 49° about $[\bar{2}\,\bar{3}\,0]$ from 12/13; secondly, the grain that includes sub-grains 14, 15, 16, 17, 18, 19, 22 and 23, this is again about 50° from 12/13 but about a different axiz $[1\,\bar{2}\,2]$; and finally, the grain on the right-hand side marked as II, whose boundary runs vertically up from the sub-grain 24. This last grain is misoriented from 12/13 by only $-17°$ about $[4\,2\,1]$. Large misorientations were found *within* the parent grain, for example 20° between 40 and 41 about a $[\bar{1}\,1\,0]$ rotation axis with a further 9° between 41 and 31 about the same rotation axis, giving a total misorientation of 29° between 40 and 31, two subgrains separated by only 3 $\mu$m. Some idea of the cumulative misorientation across the original grain can be obtained from the fact that the new

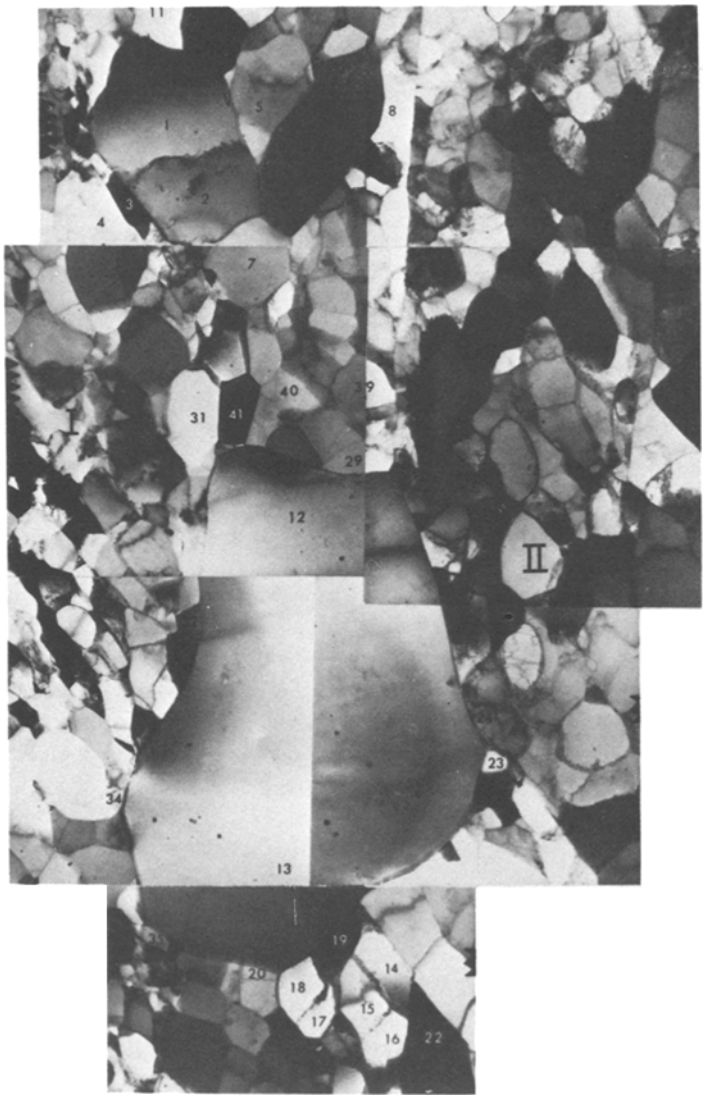


*Figure 17* Aluminium compressed 40% and annealed for 30 sec at 328° C.

grain is $-13°$ from 34 about an axis $[\bar{2}\,3\,1]$ $-7°$ from 32 about an axis close to $[\bar{1}\,1\,0]$ and from 12 to 29, is $-45°$ about $[\bar{2}\,2\,1]$, sub-grain 29 has a similar orientation to 40 which, as mentioned above, is misoriented from 31 by a rotation of $-29°$ about an axis close to $[\bar{1}\,1\,0]$ (31 to 40). From 32 to 31 is $-13°$ about a slightly different axis $[\bar{1}\,1\,3]$. Higher up the parent grain the deformation band was also detected, there is a misorientation of $-33°$ about $[\bar{2}\,1\,0]$ from 4 to 8, including 13° about $[\bar{2}\,0\,1]$ between 4 and 1, $-13°$ about $[\bar{2}\,1\,1]$ between 1 and 5 and $-17°$ about $[\bar{3}\,2\,\bar{1}]$ between 2 and 6 (6 is the black sub-grain between 5 and 8).

From this orientation information it would appear that the new grain developed from an orientation within a highly misoriented deformation band; the smallest angle is the 7° from 32, so it is most likely that the actual nucleus position lay above or below the examined foil. No trace of its origin can be made out, due to the absence of dislocations within the grain, but it is of interest to note that at the deformation band a coalescence event can be seen between sub-grains 1 and 2 that are only misorientated by 0.2°. It can also be seen that many of the sub-grains in this region of the deformation band are larger than average (1, 2, 4 to 7).

Other examples of apparent coalescence can be found at the bottom of the micrograph. Sub-grains 17, 18 and 19 are all misoriented by less than 1° (17/18 is 0.3° and 18/19 is 0.6°). So are sub-grains 14, 15 and 16 (14/16 is 0.3° and 15/16 is 0.6°). These groups of nearly coalesced sub-grains have highly misoriented neighbours, 18 is on a high-angle boundary with sub-grains 20° (18/20 is 54°) with incipient deformation bands between the two groups (19/15 is 12° about $[\bar{1}\,1\,1]$) and between 16 and 22 (5° about $[\bar{1}\,0\,\bar{2}]$). The high-angle boundary with 12, 13 is likely to be a transient effect as the new grain is growing into the sub-grain groups.

Finally, it is interesting to note, from the shape of the new grain, that it is apparently growing easily into the two lower grains with which it is strongly misoriented, 35–20 and 18–23, but that less growth has occurred into the grain, II, from which it is only misoriented by 17°. The new grain is also growing easily into part of its parent grain 29 to 41, that with which it is strongly misoriented but not into the regions of lower misorientation, for example sub-grain 32. These observations are not unexpected, given the low mobility of low- to medium-angle boundaries (31).

In the three cases where SIBM nucleation has been identified in this part of the investigation (Figs. 14, 15 and 17), the initial part of the growth of the new grain appears to have occurred in the parent grain *before* the sub-grain has gained a sufficient size advantage to be able to grow into the sub-grains on the opposite side of the pre-existing grain boundary. Many examples of sub-grain coalescence have been obtained, and in almost every case it was only found at grain boundary/deformation band intersections though in a few cases coalescence was found within deformation bands not actually on pre-existing grain boundaries (sub-grains 1/2, Fig. 17). The evidence that SIBM, in aluminium deformed 40%, occurred as suggested [10] after grain-boundary coalescence was, however, only indirect. Firstly, sub-grain coalescence could be observed at grain boundaries giving the coalesced grains a local size advantage, this coalescence occurred only where deformation bands were found. Secondly, all the successful SIBM "nuclei" were found growing from parent grains that contained deformation bands. For direct evidence of the model we would need to section the sample through the new grain at the coalesced position and before the coalescence had gone to completion, an unlikely event for well-developed nuclei.

### 4.2.2. Material compressed 60%

Samples were annealed at 250° C for times of 20 sec and 2 min to produce observable nucleation events. This temperature is some 80° C below that required for the onset of nucleation after 40% compression. Even after such brief anneals at the lower temperature some new grains were so fully developed that their origin could not be easily studied. This rapid nucleation at 250° C is not surprising given the high misorientation and incipient nucleation (Fig. 12) seen after room temperature deformation. In order to study the nucleation processes after the higher strain, regions were selected for detailed study in which nucleation was only just beginning – this allowed the microstructure of the adjacent deformed material to be studied before it was fully consumed by the growing new grains. Four regions were examined in some detail and in every case the new grain was found to be associated with a deformation band; in three cases at grain interior sites and in one case (Fig. 18), at a deformation band close to a pre-existing grain boundary. With the large local misorientations produced by the higher strain it was not easy to determine if a sharply misoriented region was associated with a pre-existing grain boundary or a deformation band. Two pieces of evidence were normally used to try to answer this question. First, the method previously used was again employed – the existence of intermediate orientations between the extremes was taken as good evidence for a deformation band [3, 4]. Secondly, the TEM foils were observed by optical microscopy after detailed TEM study and the position of the contamination spot located with respect to the original grain boundaries that could be seen, (Fig. 1, the region also shown in Fig. 19).

In Fig. 18, however, a pre-existing grain boundary was confirmed by optical microscopy. The boundary runs across the micrograph and is located between 2 and 15, and between 1 and 15, 14, and 13, with sub-grains 12 and 11 within the lower grain. The well-developed sub-grain 1 is seen to be bulging into the upper grain but is still longer *along* the boundary than into the neighbouring grain – a feature characteristic of the proposed grain-boundary coalescence model [10]. The hypothesis of coalescence is also supported by the almost decomposed sub-structure indicated by the

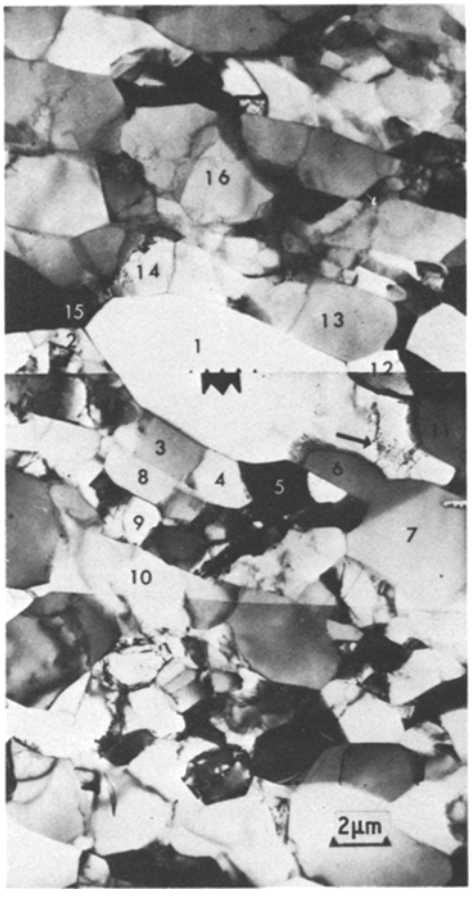


*Figure 18* Aluminium compressed 60% and annealed for 2 min at 250° C.

arrow. Sub-grains 6 and 11 also have quite low misorientations from 1 (1/6 is 2.5° and 1/11 is 3.6°).

The misorientations across the pre-existing grain boundary are as follows:

15/2 34° about $[\bar{1}\,1\,0]$

14/1 35° about $[\bar{2}\,1\,\bar{1}]$

13/12 39° about $[\bar{2}\,1\,\bar{1}]$.

Within the lower grain sub-grains, 6, 11 and 12 are quite close in orientation to new grain 1 (2.5°, 3.6° and 5.6° respectively) but other sub-boundary angles are larger:

1/2 21° about [0 1 2]

1/3 19° about [1 2 3]

1/4 18° about [1 2 2]


*Figure 19* Aluminium compressed 60% and annealed for 2 min at 250° C.

1/5 15° about [1 1 2]

1/7 14° about $[\bar{1}\,1\,2]$.

The boundary between 3 and 8 had also an above average misorientation: −8.5° between 3 and 8 – a rotation in the opposite sense than that from 1 to 3, making 8 less misoriented from 1 than was 3.

The structure seen in Fig. 18 is similar to that commonly seen after the lower strain – a SIBM bulge developing from an apparently coalesced group of sub-grains that has developed at the junction of a deformation band (or at least a very high local misorientation) and a pre-existing grain boundary.

The remaining examples of nucleation after the higher strain are all at grain interior deformation band sites. Fig. 19 shows one example where sub-grains 3 and 9 have grown larger than their neighbours and are apparently growing in at least some directions, for example 9 appears to be growing into 14, 8 and 13. Tilting experiments revealed some residual dislocations in sub-grain 3 but not in 9. Both sub-grains lie within a strongly misoriented deformation band as shown by the following misorientations.

Sub-grain 9:

11/10 11° about [2 1 4]

9/8 40° about [3 1 4]

9/14 20° about [1 1 3]

14/8 23° about [1 0 1]

9/13 42° about [2 1 4]

8/7 7° about [2 1 2].

There is a total misorientation across the band between 11/7 of 61° about an axis close to [2 1 3].

Sub-grain 3:

1/2 6° about [3 2 4]

3/4 7° about [1 0 1]

4/5 33° about [1 1 2]

5/6 3° about [0 2 1].

There is a total misorientation across the region of 48° about [1 1 2] from sub-grain 1 to sub-grain 6.

The alternative explanation is that these high misorientations are due mainly to a postulated high-angle grain boundary that might have been between 4 and 5 and between 9 and 8, and between 9 and 13. This suggestion is disproved by the existence of the intermediate orientation of sub-grain 14 and by the subsequent observation of the region by optical microscopy (Fig. 1). In Fig. 1 the contamination spot appears to be well removed from the two adjacent grain boundaries. There is no direct evidence from the microstructure around either 3 or 9 that they might have evolved by coalescence but coalescence appears to be occurring between 19 and 18 that are misoriented by only 1.7°, and the boundary between 2 and 3 is also much smaller than average – only 1.9°.

More convincing evidence of the role of coalescence in the nucleation of recrystallized

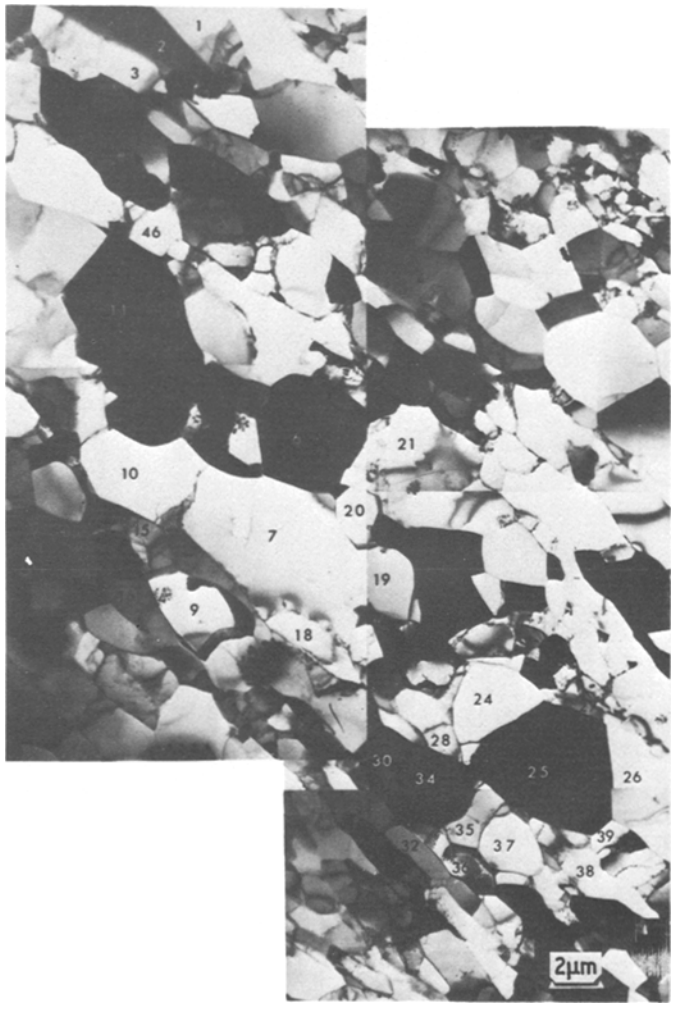


*Figure 20* Aluminium compressed 60% and annealed 20 sec at 250° C.

grains was obtained from material annealed only 20 sec at 250° C. The clearest micrographical evidence for coalescence in nucleation after 60% compression is found in a micrograph that has already been published in review articles (Fig. 16 of [27] and Fig. 25 of [28]), and need not be reproduced again here. The published micrograph showed a group of coalesced sub-grains, misoriented by only 3° over 25 μm *along* a deformation band across which there was a high local misorientation. Another example is shown in Fig. 20 in which an elongated sub-grain is seen, 7, that contains within itself a trace of an original, 1 μm, sub-grain. The boundary between 7 and 10 (1.5° misorientation) is disintegrating and there is also a low misorientation between 7 and 18 (0.9°). The elongated sub-grain lies *along* a deformation band as can be seen from the following data:

$$6/7 \quad 20^\circ \text{ about } [\bar{1}\,1\,3]$$
$$7/16 \quad 9^\circ \text{ about } [\bar{1}\,\bar{1}\,3]$$
$$21/20 \quad 7^\circ \text{ about } [\bar{1}\,\bar{1}\,3]$$
$$20/7 \quad 12^\circ \text{ about } [\bar{1}\,\bar{1}\,3].$$

Sub-grain 16 lies between 9 and 18. Despite this continuity of rotation, other local high misorientations are not cumulative; for example:

$$46/11 \quad 28^\circ \text{ about } [0\,1\,3]$$
$$11/10 \quad -20^\circ \text{ about } [0\,3\,2],$$

and across the whole band 4 to 16 there is a misorientation of only 18° about $[\bar{1}\,1\,2]$.

In the lower part of the micrograph, the group of sub-grains 30, 34, 35, 36 and 37 have almost the same orientation (30/34 0.7°, 34/35 1.6°, 35/36 0.8° and 36/37 1.0°); across this group of apparently almost coalesced sub-grains the misorientations are much larger:

$$28/30 \quad -9^\circ \text{ about } [0\,\bar{3}\,1]$$
$$30/31 \quad 20^\circ \text{ about } [0\,\bar{3}\,1]$$
and $$25/35 \quad -9^\circ \text{ about } [0\,\bar{3}\,1]$$
$$35/32 \quad 23^\circ \text{ about } [1\,\bar{3}\,2].$$

But across the whole band the misorientation is only

$$27/32 \; 13^\circ \text{ about } [\bar{1}\,\bar{1}\,3].$$

In both these examples coalescence has either occurred (sub-grain 7) or is occurring (sub-grains 30, 34–37) by the disappearance of low-angle boundaries that lie mainly at right angles to high-angle boundaries – this will give elongated sub-grains with a size advantage to the neighbouring regions from which they are separated by medium- to high-angle boundaries – which should be highly mobile [31]. In the previously published structure [27, 28] the growth of the elongated sub-grain had started before coalescence was complete.

### 4.2.3. Heavily rolled aluminium foil

Some commercial aluminium foil rolled to 98% reduction in thickness was kindly supplied by Alcan Laboratories and this was examined by TEM in the as-rolled condition and after an anneal of 10 min at 250° C. The structures observed, in sections parallel to the rolling plane, showed a small equi-axed sub-grain structure (0.5 to 2 μm in size) after rolling. After annealing some general sub-grain growth was observed (Fig. 21), with the sub-grains 2 to 4 μm in size, but with the occasional larger sub-grain up to 10 μm in size. One such enlarged sub-grain can be seen in Fig. 21 and its microstructure suggests that it is composed of several nearly coalesced sub-grains, 1, 2, 3, 4 and 13. This was confirmed by the Kikuchi analysis which revealed the following small misorientations:

$$1/3 \quad 0.3^\circ$$
$$1/4 \quad 0.4^\circ$$
$$2/3 \quad 0.7^\circ$$
$$4/13 \; 0.6^\circ.$$

Other very low angles characteristic of coalescence are:

$$7/8 \quad 0.5^\circ$$
$$14/15 \; 0.5^\circ.$$

Apart from low-angle boundaries all the other boundaries had misorientations of 6° or more (apart from 5/6 of only 3°). These measurements strongly suggest a coalescence mechanism which is further supported by the observation of some high misorientations characteristic of deformation bands especially near to the main sub-grain group of 1, 2, etc.,

$$2/9 \quad 40^\circ \text{ about } [\bar{1}\,\bar{1}\,1]$$
$$8/9 \quad 52^\circ \text{ about } [\bar{2}\,\bar{2}\,1]$$
$$4/6 \quad 23^\circ \text{ about } [\bar{3}\,\bar{3}\,\bar{1}]$$

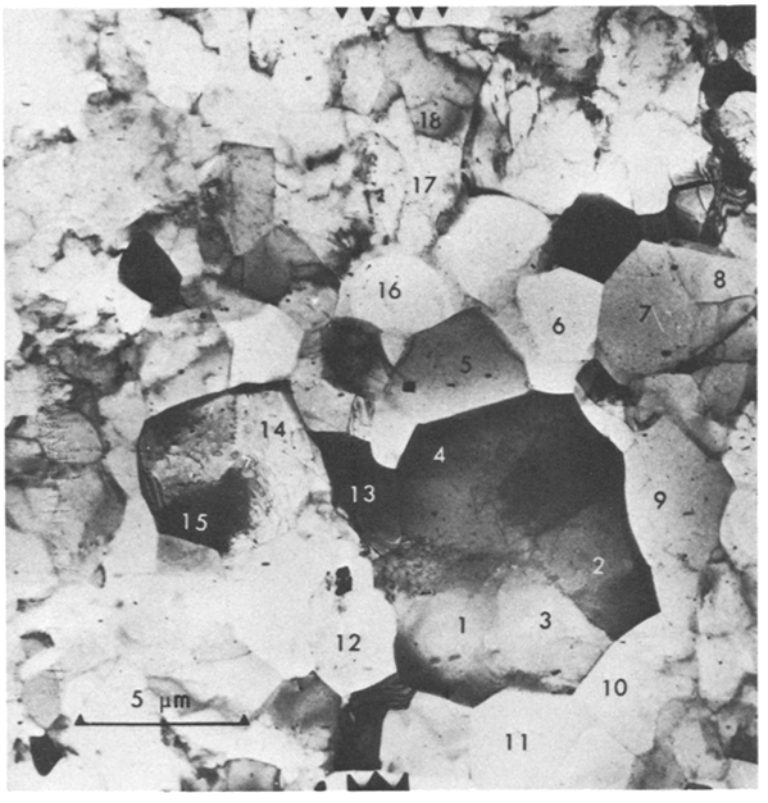


*Figure 21* Commercial aluminium foil cold rolled 98% and annealed for 10 min at 250° C. Rolling plane section.

18/17 16° about $[\bar{1}\,\bar{1}\,1]$

4/5 −18° about $[\bar{1}\,\bar{1}\,\bar{1}]$

12/1 12° about $[\bar{1}\,\bar{2}\,0]$

12/13 12° about $[\bar{1}\,\bar{2}\,0]$

14/13 8° about $[\bar{2}\,\bar{1}\,\bar{2}]$.

The range of rotation angles about a nearly common rotation axis strongly suggests a deformation band, but with only a very limited investigation of the misorientations and structures in the heavily rolled foil, it is not possible to be certain if this is a deformation band or a pre-existing grain boundary. However, it is clear that the coalescence process seen is again occurring preferentially near very high local misorientations.

## 5. Discussion of results

### 5.1. Statistical analysis of the deformed and partially recrystallized material

From the samples examined, the following data was obtained for sub-grain sizes (Table I) and sub-boundary angles (Figs. 22 and 23 and Table II). It is clear from these data that there is general sub-grain growth on annealing, in addition to the specific sub-grain coasening events associated with nucleation. The misorientation data show several interesting effects; these include the expected increase of the mean misorientation with increased strain [28] and more particularly the increase of both the average misorientation and the spread of misorientation on annealing. The wider spread of angles after annealing is precisly what would be expected if sub-grain coalescence was occurring. The low-angle boundaries should become less misoriented while the higher angle boundaries should increase their misorientation [9]. However, this evidence must be treated with some caution since the way the regions were selected for analysis was different in the as-deformed state and after annealing. In the as-deformed material the regions

TABLE I

| | Sub-grain sizes (μm) |
|---|---|
| 40% compression | 1.0 |
| Annealed for 30 sec at 328° C | 1.4 |
| 60% compression | 1.0 |
| Annealed for 20 sec at 250° C | 1.5 |

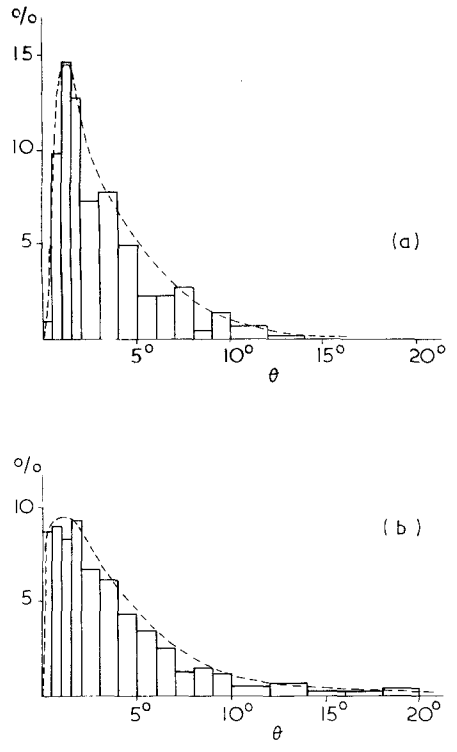


*Figure 22* Distribution of sub-boundary misorientations in aluminium compressed 40% (a) as-deforemd, and (b) after brief annealing (10 and 30 sec) at 328° C.

TABLE II Distribution of sub-grain misorientations (Figs. 22 and 23)

| | $\theta_{max}$ | $\bar{\theta}$ | $\sigma$ | $N$ |
|---|---|---|---|---|
| 40% Compression | 1.5° | 3.6° | 3.1° | 113 |
| Annealed at 328° C | 1.2° | 4.3° | 4.2° | 333 |
| 60% Compression | 3.0° | 5.0° | 4.3° | 37 |
| Annealed at 250° C | 1.7° | 8.2° | 6.1° | 172 |

$\theta_{max}$ is the maximum in the distribution
$\bar{\theta}$ is the average misorientation
$\sigma$ is the standard deviation of the distribution and
$N$ is the number of boundaries examined.

examined were selected at random while in the partially recrystallized material the regions were selected for examination if they contained regions showing preferential sub-grain growth or nucleation. That the average misorientation is higher after annealing may merely indicate that somewhat different regions were examined before and after annealing. On this basis it is probably safest to consider that the wider spread of misorientation after annealing is most likely due to the fact that nucleation occurs preferentially in areas with a larger spread of misorientation: a somewhat limited conclusion, but one that still

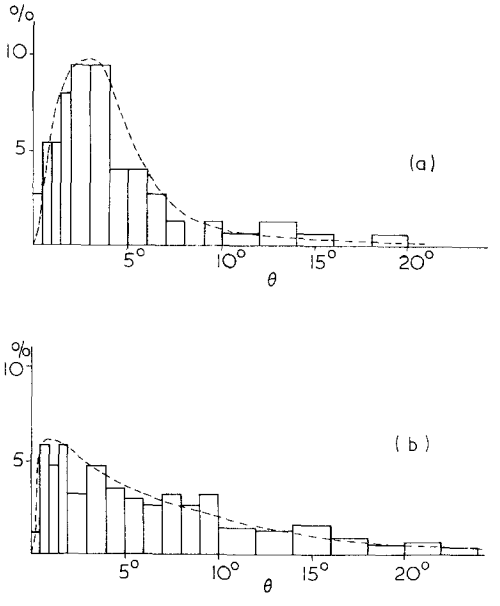


*Figure 23* Distribution of sub-boundary misorientations in aluminium compressed 60%. (a) as-deformed, and (b) after brief annealing (20 sec and 2 min) at 250° C.

supports the suggestion of sub-grain coalescence as the mechanism of nucleation in the material examined. A subsequent study by Kriesler and Doherty [18] was able to study the same deformation band before and after annealing. This also supported coalescence as the nucleation mechanism.

Using the average values of the mean misorientation we can obtain an estimate of the stored energy in the deformed material due to the sub-boundaries. The stored energy, $\Delta E$, is given by:

$$\Delta E = \frac{N}{2} \sum_{i=0}^{i=N} A\gamma(\theta) = \frac{1}{2V} \sum_{i=0}^{i=N} A\gamma(\theta),$$

where $\gamma(\theta)$ is the sub-boundary energy at a misorientation $\theta$, $A$ is the area of the $i$th sub-grain, $N$ is the number of sub-grains per unit volume, and $V$ is the mean sub-grain volume. Assuming that $\gamma(\theta)$ is proportional to $\theta$, which is a reasonable approximation for angles less than 10° [32], gives $\Delta E = A\gamma(\theta)/2V$. Taking $A$ as $4\pi r^2$ and $V$ as $4\pi r^3/3$ with $2r$ the sub-grain diameter, gives:

$$\Delta E \approx 3\gamma(\bar{\theta})/2r.$$

$\gamma(\bar{\theta})$ can be estimated from the results of Gjostein and Rhines [32] for copper, corrected by the ratio of the shear moduli of aluminium to that of copper.

After 40% compression $\bar{\theta} = 3.6°$ so $\gamma(\bar{\theta}) = 0.14\,J\,m^{-2}$, and after 60% compression $\bar{\theta} = 5.0°$ so $\gamma(\bar{\theta}) = 0.17\,J\,m^{-2}$. Taking $r$ as $0.5\,\mu m$ and the molar volume of aluminium as $10^{-5}\,m^3\,mol^{-1}$ gives:

$$40\%\text{ compression } \Delta E = 4\,J\,mol^{-1}$$

$$60\%\text{ compression } \Delta E = 5\,J\,mol^{-1}.$$

These figures are less than half the value for stored energy reported by Åstrom [33] for compressed aluminium, ($11\,J\,mol^{-1}$ after 45% compression). The discrepancy might be due to the slightly purer material of the present study (99.997%) as against the 99.99% used by Åstrom. A more likely conclusion, however, could be that the dislocation arrangements in the low-angle sub-grain do not represent the equilibrium dislocation arrangement. This idea could then partially account for the considerable softening that is found on annealing deformed aluminium before recrystallization occurs (e.g. [34–36]). The sub-boundary dislocation arrays after deformation could relax to contain only the "geometrically necessary" dislocations [37] to make up their misorientation by the mutual annhilation of the "statistically stored" dislocations. A full study of this possibility would need careful determination of the details of the release of stored energy from the deformed material before the onset of recrystallization.

## 5.2. Microstructure of the deformed material and microstructural change in annealing

The significance of the observations has already been discussed in the results section and only the main conclusions need to be summarized here. The deformation bands [1] seen by optical microscopy could not be identified by TEM in the as-deformed material. High misorientation was, however, found across individual sub-boundaries as high as 13° (40% compression) and 19° (60%). After annealing, the preferential growth of sub-grains in regions of high local misorientation allowed the highly misoriented deformation band regions to be detected and studied, this was also the case in one example (Fig. 12), where incipient nucleation was detected in the as-deformed material. The structure of the deformation bands seen in the present material differs in two respects from that previously reported [3, 4]. Firstly, the rotations right across the highly misoriented bands were often only partially cumulative; that is the material after rotation away from a matrix orientation would often rotate back towards the original orientation. This present observation also contrasts with the type of banding previously found for coarse grained aluminium [1] in which the deformation bands separated large regions each with widely differing orientations. The same geometry was reported for rolled iron-based material [3, 4, 20] although the compressed iron studied by Inokuti and Doherty [21] showed finely interspersed bands of differing orientation in which orientation rotated back and forth. A further difference from the earlier observations [3, 4] was the fine structure of the deformation bands. The earlier studies reported thin *elongated* sub-grains within the deformation band. In the pesent study, the deformation bands seen albeit after some brief annealing, had *equi-axed* sub-grains. The as-deformed microstructure showed the elongated columnar sub-grain structure in many parts of the deformed grains, with low angles along the columns and, in general, higher boundary angles across the columns. The columnar structure was not specific to deformation bands. On annealing, the columnar appearance of the *general* microstructure disappeared with most of the sub-grains becoming equi-axed (Figs. 13 to 20). However, within some deformation bands and along some grain boundaries, isolated groups of sub-grains often formed elongated sub-grains (Figs. 14, 18 and 20, and in Fig. 16 of [27]), a feature that provided characteristic evidence, with the orientation measurements for sub-grain coalescence. The disappearance of the regions of columnar sub-grains as a *general* feature of the microstructure suggests that sub-boundary migration, [4, 19] is the main mechanism of general sub-grain growth. This conclusion, of general sub-grain growth by migration rather than by coalescence, was reached, albeit by different evidence, for the recovery processes in rolled iron by Dillamore and Smith [38].

The localized and preferential growth of some sub-grains, leading to nucleation, found in the present study indicates, very strongly, that sub-grain coalescence is a significant nucleation mechanism. As previously discussed [27, 28] for nucleation a sub-grain needs to be larger than its neighbours and to have, or quickly acquire a high angle (high mobility) boundary [31]. The fact that sub-grain coalescence appears, in the present

work, to occur only at positions of high local misorientations, strongly favours the coalescence model of nucleation [3]. Coalescence of sub-grains then creates precisely the required microstructure for nucleation – a significantly larger sub-grain [10] adjacent to a high misorientation – either at a grain boundary, giving SIBM, or in a grain interior at a deformation band [1, 20, 21].

Bailey and Hirsch [7] developed a model for SIBM, in which a dislocation-free sub-grain of length $2L$ along the pre-existing high-angle grain boundary, can bulge into the neighbouring unrecovered grain whose stored energy is $\Delta E$. The condition for successful nucleation is that the bulge grows beyond the minimum radius of curvature – the hemisphere of diameter $2L$. The relevant relationship is:

$$L \geqslant 2\gamma_g/\Delta E$$

where $\gamma_g$ is the grain-boundary energy.

A similar analysis to that of Bailey and Hirsch can be readily performed for a high stacking fault energy material like aluminium, in which after the briefest anneal the dislocation structure is polygonized into almost dislocation-free cells. A sub-grain along a pre-existing grain boundary has become enlarged within its own grain, by coalescence (or some other process) to give length $2L$ along the boundary; all the other sub-grains have a diameter of $2r$ (Fig. 24a). The sub-grain boundaries have an energy $\gamma_s$, which after some recovery should be the equilibrium energy for boundaries with the measured misorientation [32].* This idea has already been discussed with respect to the stored energy. The balance of boundary tensions will determine the equilibrium triple point angle $2\phi$ (Fig. 24b) with $\cos\phi = \gamma_s/2\gamma_g$. The curvature of the high-angle grain boundary produced by these triple point angles will cause initial bulging (Fig. 24c). The critical condition for SIBM nucleation [7] will be determined by the hemispherical shape of the bulge, as nucleation will be possible if, at the approximately hemispherical condition (Fig. 24d), the curvature of the grain boundary is still convex towards the enlarged sub-grain, or if the boundary segments are flat. The condition for SIBM nucleation is then:

$$L \geqslant r/\cos\phi = 2r\gamma_g/\gamma_s.$$

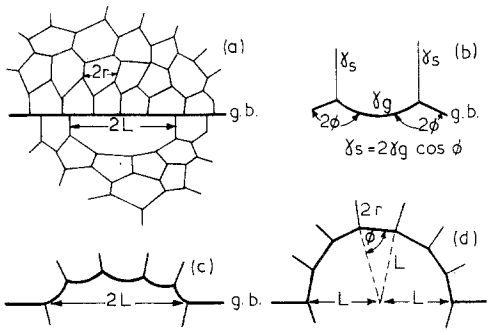


*Figure 24* Model of strain-induced boundary migration in well polygonized material.

For the grain growth problem, where $\gamma_s = \gamma_g$, $L = 2r$, giving the condition for the continued growth of one large grain without any movement of other grain boundaries (secondary recrystallization or abnormal growth [39]). For material in the present investigation with sub-boundaries of about 3° misorientation, the value of $\gamma_g/\gamma_s$ for fcc material is $\approx 3$ [32] and with $2r = 1.4\,\mu$m we obtain:

$$2L \geqslant 7\,\mu\text{m}.$$

In all the examples of successful SIBM nucleation seen in this study (Figs. 14 and 16 to 18), this condition is fulfilled and in the case where coalescence was detected but bulging had not occurred, the value of $2L$ was $5\,\mu$m or less (Fig. 15, and Fig. 15 of [27]). A similar analysis should be appropriate for sub-grains at highly misoriented deformation bands – though a further sub-grain coalescence or migration stage might be required for the boundaries parallel to the deformation band to acquire sufficient misorientation to be high-angle, and therefore mobile, grain boundaries [31].

The sub-grain coalescence processes seen in the present study show that adjacent sub-grains of 1 to $2\,\mu$m diameter can rapidly coalesce. The observed times for the process can be readily compared with the predictions of Li's model for coalescence by dislocation climb and by glide [9]. For the rotation of two sub-grains of diameter $2L$ by the climb of edge dislocations (tilt component) the time $t$, for the disappearence of a sub-boundary of misorientation of about 2°, is given by:

$$t = L^2\, kT/3DE_0b_j^3$$

*At an earlier stage in the annealing process, the energy might be larger than the equilibrium value if the sub-boundary has more dislocations than are "geometrically necessary" [37] to make up the measured misorientation, or if the dislocations have not arranged themselves into the minimum energy configuration.

where $D$ is the diffusion coefficient ($D = 1.7 \times 10^{-4} \exp(-34\,000/RT)\, m^2/8$ [40]), $E_0$ is $Gb/4\pi(1-\nu)$, $G$ is the shear modulus $2.3 \times 10^{10}$ pa, $b$ the Burgers vector of the dislocations $2.9 \times 10^{-10}$ m, $\nu$ is Poissons' ratio 0.34 and $j$ is the jog density, in which we have followed Li [9] in taking as the very high value of $1/3b$ and $k, R$ and $T$ have their usual significance. The calculated times (for $L = 1\,\mu$m) are found to be 23 h at 250° C and 20 min at 328° C – *much* longer than the observed annealing times (20 sec and 2 min at 250° C (60% compressed aluminium), 10 min at 250° C (rolled commercial aluminium) and 10 to 30 sec at 328° C (40% compressed aluminium)).

Li [9] also gives an equation for the rate of rotation of two sub-grains that are coalescing by glide of screw dislocations (twist component). This rate of rotation gives the following equation for the time for complete coalescence of two sub-grains, misoriented by a 1 to 2° *twist* boundary:

$$t \approx 2L^2 j_s kT/3DE_0 b.$$

The jog density, $j_s$, for the screw dislocations was estimated using the relationship given by Friedel [41]:

$$j_s = \exp(-U_j/kT)/b$$

with $U_j = Gb^3/10 = 0.35$ eV

giving $j_s$ of $4 \times 10^{-4}/b$ at 250° C

and $j_s$ of $1 \times 10^{-3}/b$ at 328° C.

This gives very much more rapid coalescence, 20 sec at 250° C and 1 sec at 328° C. (If we used the very high values of $j_s$ previously assumed for climb ($j = 1/3b$) this greatly increases the calculated times.) The implicaton of the approximate agreement between these calculated times with the observed coalescence results is either that Li's model for sub-grain coalescence by dislocation climb is incorrect or that only sub-boundaries with a largely twist component were being eliminated. It was not found possible with foils only 100 to 200 nm thick to determine the spatial orientation of boundaries between sub-grains 2 to 5 $\mu$m diameter. The problem of which type of boundaries are involved in coalescence is one that will need further experimental study. Such a study may be most effectively carried out by the use of thicker foils studied by high voltage electron microscopy so the orientation of the boundary plane, with respect to the rotation axis, can be determined. Such a study combined with direct HVEM observation during *in situ* heating [19, 42] would also allow direct determination of the kinetics and possibly the mechanisms of sub-grain coalescence.

## 6. Conclusions

(1) Aluminium, with a grain size of 80 $\mu$m, recrystallizes after 20 and 40% compression by stain-induced boundary migration (SIBM) and after 60% compression by grain interior nucleation.

(2) Optical microscopy revealed strongly misoriented deformation bands in the material after strain and the process of SIBM was seen in many cases to be associated with deformation bands in the parent grain.

(3) Transmission electron microscopy, TEM, showed in the section parallel to the compression axis a "columnar" sub-structure with lower misorientations along the columns and a higher misorientation across the columns. Misorientations close to grain boundary triple points showed a mixture also of high and low misorientations.

(4) Attempts to find deformation bands in the as-deformed material by TEM were not successful, except in one case after 60% compression where the deformation band was shown up by incipient nucleation in the (room temperature) deformed material, a possible case of dynamic nucleation.

(5) Lightly annealed material showed evidence, by micrographic appearance and misorientation measurements for sub-grain coalescence. This was not a general recovery sub-grain growth process as it occurred only in regions of high local misorientation. Such regions were identified as deformation bands and deformation band/grain boundary junctions.

(6) Nucleation of recrystallization was identified as occurring by the growth of sub-grains, enlarged by coalescence, into regions from which they were highly misoriented, by more than 20°.

(7) The kinetics of the coalescence process occurred much faster than predicted for a dislocation climb mechanism but at a rate more compatible with glide of screw dislocation, a mechanism for the disappearance of low-angle twist boundaries only.

(8) The calculated stored energy, assuming that the sub-boundaries had the equilibrium dislocation structure, underestimated the previously measured values by more than 50%. The discrepancy could be due to the statistically stored dislocations in the as-deformed sub-boundaries.

## Acknowledgements

The authors are grateful to Professor R. W. Cahn for encouragement of this research, provision of facilities and for many useful discussions; to Dr R. Pond for the technique of producing electron microscope specimens; to Alcan Laboratories for provision of material and to Dr S. P. Bellier, Dr W. B. Hutchinson, Dr P. L. Morris, Dr A. Kriesler and Professor I. L. Dillamore for useful discussions. One of us (P. F.) would like to thank the Centre National de la Recherche Scientifique and the Royal Society for financial support.

## References

1. S. P. BELLIER and R. D. DOHERTY, *Acta Met.* **25** (1977) 521.
2. C. S. BARRETT, "Structure of Metals" (2nd Edn. McGraw Hill, 1952) pp. 372, 453.
3. H. HU, "Recovery and Recrystallization of Metals", Edited by L. Himmel, (Gordon and Breach, New York, 1963) p. 311.
4. I. L. DILLAMORE, P. L. MORRIS, C. J. E. SMITH and W. B. HUTCHINSON, *Proc. Roy. Soc.* **329A** (1972) 405.
5. G. I. TAYLOR, *J. Inst. Metals* **62** (1938) 307.
6. P. A. BECK and P. R. SPERRY, *J. Appl. Phys.* **21** (1950) 150.
7. J. E. BAILEY and P. B. HIRSCH, *Proc. Roy. Soc.* **267A** (1962) 11.
8. H. FUJITA, *J. Phys. Soc. Japan* **16** (1961) 397.
9. J. C. M. LI, *J. Appl. Phys.* **33** (1962) 2958.
10. R. D. DOHERTY and R. W. CAHN, *J. Less Common Metals* **28** (1972) 279.
11. R. H. GOODENOW, *Trans. Quart. ASM* **59** (1966) 804.
12. N. RYUM, *Acta Met.* **17** (1969) 831.
13. J. W. EDINGTON, "Practical Electron Microscopy in Materials Science" Vol. 2, (Macmillan, 1975).
14. R. POND, private communication.
15. P. FAIVRE, D. Phil. Thesis, University of Sussex (1973).
16. A. W. AGAR, *Brit. J. Appl. Phys.* **11** (1960) 185.
17. P. FAIVRE, *J. Appl. Crystallogr.* **8** (1975) 356.
18. A. KRIESLER and R. D. DOHERTY, *Metal Sci* (to be published).
19. R. K. RAY, W. B. HUTCHINSON and B. J. DUGGAN, *Acta Met.* **23** (1975) 831.
20. Y. INOKUTI and R. D. DOHERTY, *Texture* **2** (1977) 143.
21. *Idem, Acta Met.* **26** (1978) 61.
22. J. E. HILLIARD, "Recrystallization, Grain Growth and Texture", (ASM Metals Pal. Ohio. 1966) p. 267.
23. S. P. BELLIER, D. Phil. Thesis, University of Sussex (1971).
24. W. A. JOHNSON and R. W. MEHL, *Trans. AIME* **135** (1939) 416.
25. J. W. CAHN, *Acta Met.* **4** (1956) 449.
26. J. H. CAIRNS, J. CLOUGH, M. A. P. DEWEY and J. NUTTING, *J. Inst. Metals* **99** (1971) 93.
27. R. D. DOHERTY, *Metal Sci. J.* **8** (1974) 132.
28. R. D. DOHERTY, in "Recrystallization of Metallic Materials", 2nd Edn. Edited by F. Haessner (Rieder-Verlag, Stuttgart, 1978).
29. K. T. AUST and J. W. RUTTER, "Recovery and Recrystallization of Metals", edited by L. Himmel (Gordon and Breach, New York, 1963) p. 131.
30. K. LÜCKE, R. RIXEN and M. SENNA, *Acta Met.* **24** (1976) 103.
31. R. VISWANATHAN and C. L. BAUER, *ibid.* **21** (1973) 1099.
32. N. A. GJOSTEIN and F. N. RHINES, *ibid.* **7** (1959) 319.
33. H. U. ÅSTOM, *ibid.* **3** (1955) 508.
34. E. C. W. PERRYMAN, *Trans. AIME* **203** (1955) 1053.
35. R. E. DOHERTY and J. W. MARTIN, *J. Inst. Metals* **91** (1963) 332.
36. R. D. DOHERTY, Thesis, Department of Metallurgy, University of Oxford (1964).
37. M. F. ASHBY, *Phil. Mag.* **21** (1970) 399.
38. C. J. E. SMITH and I. L. DILLAMORE, *Metal Sci. J.* **4** (1970) 161.
39. J. W. MARTIN and R. D. DOHERTY, "Stability of Microstructure in Metallic Systems" (C. U. P. 1976) p. 236.
40. T. S. LUNDY and J. F. MURDOCH, *J. Appl. Phys.* **33** (1963) 1671.
41. J. FRIEDEL, "Dislocations" (Pergamon Press, 1964) pp. 109 and 297.
42. W. ROBERTS and B. LEHTINEN, *Phil. Mag.* **26** (1972) 1153.

Received 17 May and accepted 31 August 1978.